

## Sensing properties of assembled $\text{Bi}_2\text{S}_3$ nanowire arrays

This content has been downloaded from IOPscience. Please scroll down to see the full text.

2015 Phys. Scr. 90 094017

(<http://iopscience.iop.org/1402-4896/90/9/094017>)

View [the table of contents for this issue](#), or go to the [journal homepage](#) for more

Download details:

IP Address: 143.239.220.93

This content was downloaded on 18/09/2015 at 17:05

Please note that [terms and conditions apply](#).

# Sensing properties of assembled Bi<sub>2</sub>S<sub>3</sub> nanowire arrays

G Kunakova<sup>1</sup>, R Meija<sup>1</sup>, I Bite<sup>1</sup>, J Prikulis<sup>1</sup>, J Kosmaca<sup>1</sup>, J Varghese<sup>2</sup>, J D Holmes<sup>2</sup> and Donats Erts<sup>1</sup>

<sup>1</sup>Institute of Chemical Physics, University of Latvia, 19 Raina Blvd., LV-1586, Riga, Latvia

<sup>2</sup>Centre for Research on Adaptive Nanostructures and Nanodevices, Trinity College Dublin, Ireland

E-mail: [Gunta.Kunakova@lu.lv](mailto:Gunta.Kunakova@lu.lv)

Received 5 October 2014

Accepted for publication 19 March 2015

Published 13 August 2015



CrossMark

## Abstract

Bismuth sulfide (Bi<sub>2</sub>S<sub>3</sub>) nanowires were grown in porous aluminium oxide template and a selective chemical etching was applied to transfer the nanowires to a solution. Well aligned nanowire arrays were assembled on pre-patterned silicon substrates employing dielectrophoresis. Electron beam lithography was used to connect aligned individual nanowires to the common macroelectrode. In order to evaluate the conductometric sensing performance of the Bi<sub>2</sub>S<sub>3</sub> nanowires, current–voltage characteristics were measured at different relative humidity (RH) levels (5–80%) / argon medium. The response of the Bi<sub>2</sub>S<sub>3</sub> nanowires depending of RH is found to be considerably different from those reported for other types of nanowire RH sensor devices.

Keywords: nanowire array, bismuth sulfide, relative humidity

(Some figures may appear in colour only in the online journal)

## Introduction

Semiconducting nanowires have been demonstrated as promising structural elements in conductometric sensors for biological and chemical gas sensing [1, 2]. The excellent sensitivity to environmental adsorbents originates from the increased nanowire surface-to-volume ratio. Moreover, sensitivity can be tuned by nanowire dimensions, morphology and doping concentration. Recent studies show even ultra-sensitive response of nanowires operating in the so called sub-threshold regime, where the charge screening length of the nanowire is lower than its radius and can have a great surface impact to the whole nanowire volume [3].

Conductometric relative humidity (RH) sensing is an important field in the sensor industry. Ceramic materials are widely used for this purpose. Other types, including metal oxide nanowire based RH sensors have also been reported [4]. However, the humidity sensing mechanism of nanowire sensor devices may become very complex, since the water molecules can have different types of interaction with the nanowire surface, such as chemisorption, physisorption and ionic conduction at higher RH levels. Among the applications in the RH sensing devices it is important to evaluate the RH

impact on the nanostructure electrical properties for various analyte sensing at room temperature atmospheric conditions.

In this work we study bismuth sulfide (Bi<sub>2</sub>S<sub>3</sub>) nanowire sensing behaviour at different RH levels. Bi<sub>2</sub>S<sub>3</sub> is an n-type semiconductor where conduction is provided by sulfur vacancies as an intrinsic property [5] causing large variation of the resistivity. Lone pairs of electrons for both bismuth and sulfur atoms can act as active centres for donor–acceptor-like interaction resulting in an increased selectivity to the impurities or local sensitivity [6]. Combining these properties with nanometer size geometry, Bi<sub>2</sub>S<sub>3</sub> nanowires are expected to be an excellent element in sensor devices. To date, there are only few reports devoted to the Bi<sub>2</sub>S<sub>3</sub> nanowire sensor applications. This includes investigations of hydrogen, oxygen sensing and biomolecule detection [7–9]. However, detailed research on the RH impact on the Bi<sub>2</sub>S<sub>3</sub> electrical properties or application in the RH sensors has not been reported.

To provide high sensing performance and ability to functionalize nanowires for selectivity enhancement, it is advantageous to employ nanowire arrays for sensor device fabrication. Different approaches of nanowire array sensor fabrication have been demonstrated in recent years. These include dielectrophoretically aligned nanowires and

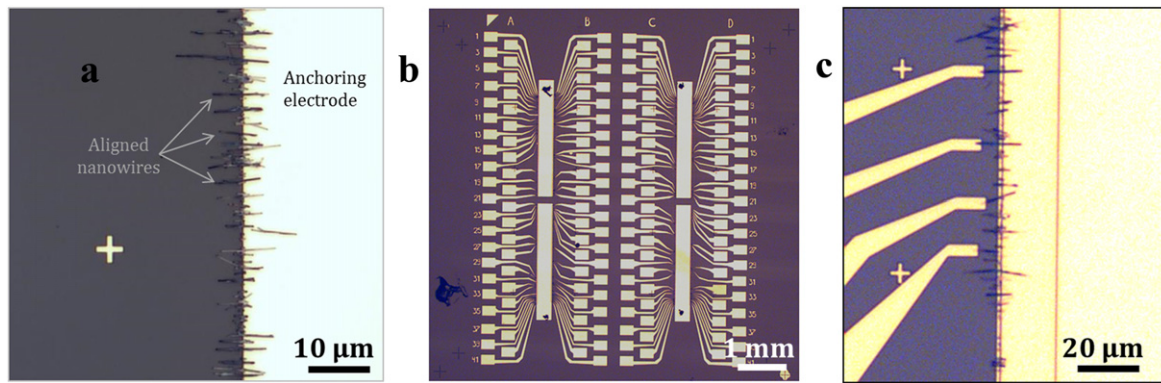


**Figure 1.** (a) Dielectrophoretically aligned individual nanowires to the macroelectrode; (b) overview of the fabricated  $\text{Bi}_2\text{S}_3$  nanowire array; (c) electrically connected individually accessible nanowires.

lithographically patterned silicon nanowire arrays [10, 11]. In the proposed solutions, nanowires cannot be accessed individually, or the surface of the fabricated nanowires can present large defect concentration.

In the present work nanowires are aligned and connected individually and partly suspended, therefore freely accessible surface area is gained, but the high density of the connected individual nanowires can be used to collect sufficient statistical data. The main focus of this study is devoted to the  $\text{Bi}_2\text{S}_3$  nanowire RH sensing properties at room temperature.

## Experimental section

Synthesis of the  $\text{Bi}_2\text{S}_3$  nanowires was carried out in a glass tube by decomposition of organometallic precursor placed on the surface of an AAO template as described in details elsewhere [12]. The surface of the  $\text{Bi}_2\text{S}_3$ /AAO nanowire membranes was polished (diamond suspension, 1–0.1  $\mu\text{m}$ ) to remove  $\text{Bi}_2\text{S}_3$  layer formed on top of the AAO. Nanowire template was dissolved using 9%  $\text{H}_3\text{PO}_4$  solution [13], nanowires were washed with deionized water and finally transferred to isopropanol using centrifugation.

n-type silicon wafer covered with  $\sim 50$  nm  $\text{Al}_2\text{O}_3$  layer grown by the atomic layer deposition was used as the substrate. Electron beam lithography (EBL) was applied for electrode patterning. Subsequently dielectrophoresis was used to align nanowires to the selected electrodes (2 MHz; 9 V). To connect individual nanowires and pattern electrodes a second EBL step was performed. Prior to metal evaporation, the contact area was cleaned using  $\text{Ar}^+$  ion etching (5 keV, 120  $\mu\text{A}$ , 10 s).

Electrical characterization was conducted in a designed custom built measurement system. The sample was located in a temperature controllable gas chamber with electronic connections and access for gas flow exchange. For conductometric RH response measurements, stable RH level from 5–80% was provided by water–glycerol solutions [14]. RH was maintained in the measurement chamber by constant argon flow (2 sccm, Ar, 99.99%) bubbling through the water–glycerol solution with different glycerol concentrations corresponding to the different RH. The actual level of the RH in

the measurement chamber was monitored by the hygrometer (HIH-4010).

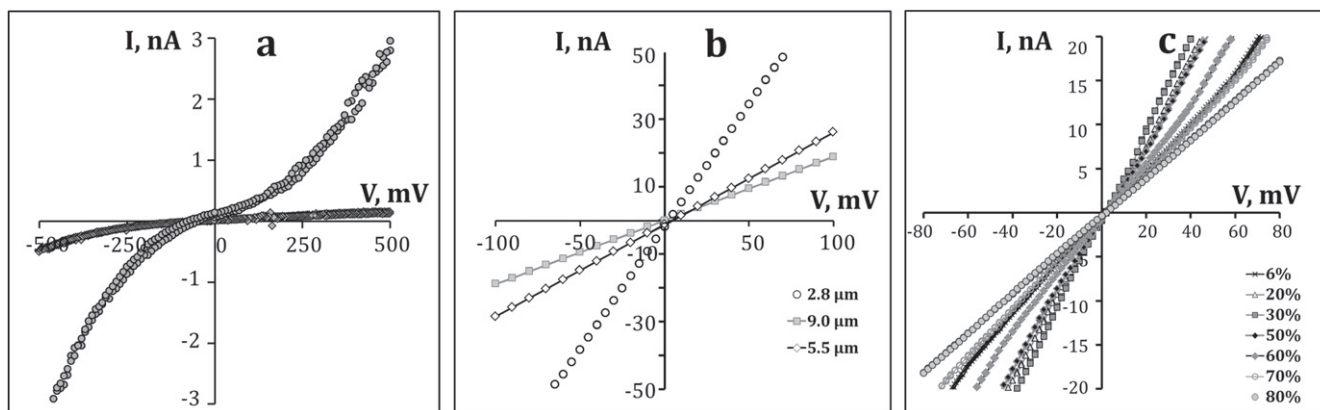
## Results and discussion

Figure 1 presents optical images of the nanowire array sensor device. The dielectrophoresis yielded perpendicularly aligned nanowires with respect to the macroelectrode. Aligned nanowires had negligible misalignment angle ( $\leq 5^\circ$ ). On average one nanowire with length exceeding 3  $\mu\text{m}$  can be found per 2  $\mu\text{m}$  line along the anchoring macroelectrode edge (figure 1(a)). Selected individual nanowires with lithographically connected contacts are shown in figures 1(b) and (c). Thus, combining dielectrophoresis and EBL, more than 100 individual nanowires were connected per chip forming a high density individually accessible  $\text{Bi}_2\text{S}_3$  nanowire array.

Current–voltage measurements for  $\text{Bi}_2\text{S}_3$  nanowires demonstrated nonlinear dependences which can be attributed to the Schottky barrier formation at the metal–semiconductor interface (figure 2(a)). For the  $\text{Bi}_2\text{S}_3$  nanowires it was reported previously as common characteristics to form a Schottky barrier [15–17]. In fact, including argon ion etching step before the metal electrode evaporation during sample fabrication, characteristics with linear dependence were obtained. Thus 90% of measured curves for all connected nanowires with etched contact area were Ohmic. Some examples of the current–voltage characteristics (IVC) are depicted in the figure 2(b).

For semiconducting nanowire with metal contacts linear IVC are highly desirable to study the sensing properties. Nanowire with nonlinear IVC provided by Schottky barrier can introduce additional effects, for example, memristive mechanism, following by pronounced hysteresis in the IVC [18]. In this work only Ohmic IVC for sensing measurements were used at low operational bias voltage ( $\pm 40$  mV).

Prior to RH sensing characterization, nanowire response to  $\text{O}_2$  and  $\text{SO}_2$  at inert atmosphere was tested. No measurable changes of the resistance were recorded after nanowire exposure to these analytes at maximum concentration of 1000 ppm, respectively. We note that in the earlier reports on  $\text{Bi}_2\text{S}_3$  nanowire sensors a considerable oxygen sensitivity was



**Figure 2.** (a) Non-linear IVC for individual  $\text{Bi}_2\text{S}_3$  nanowires; (b) IVC of the individual  $\text{Bi}_2\text{S}_3$  nanowires at inert atmosphere and low relative humidity level (RH-5%); (c) IVC for a  $\text{Bi}_2\text{S}_3$  nanowire at different RH level/argon environment,  $L_{\text{nw}} = 3.8 \mu\text{m}$ .

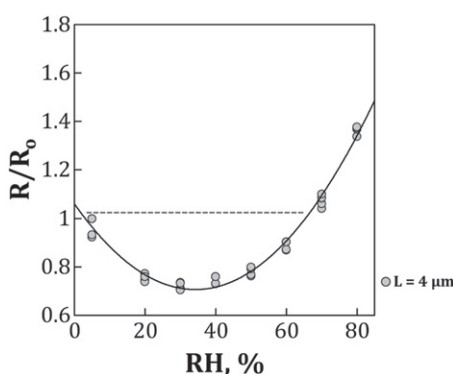


**Figure 3.** Relative humidity sensing response of the individual nanowire (bias 40 mV).

present [8]. Sensing response was recorded after exposure to air and observed decrease of resistance was considered mainly due to the oxygen chemisorption, however, the RH level in air was not monitored. In the present work we observe change of the nanowire resistance by modulating the RH level instead. Thus one can assume to have an increased nanowire selectivity to water molecule sensing for studied nanowires.

To test the nanowire sensing performance, the IVC at different RH levels up to 80% in an otherwise inert medium (argon) were measured (figure 2(c)). The IVC remained linear in all measured RH levels and change of the resistance was observed when comparing low (6%) and high (80%) RH levels.

To evaluate nanowire response to the RH, one can plot the nanowire response sensitivity as a function of RH level defining sensitivity as  $R_{\text{RH}}/R_0$ , where  $R_0$  is nanowire resistance at dry argon with RH  $\sim 5\%$  (figure 3). Obtained  $R_{\text{RH}}/R_0$  versus RH dependence had nonlinear behaviour for all measured devices, as depicted in figure 3. In fact, at the RH level around 40% nanowire response passes through a minimum. Consequently at RH 5–40%, nanowire resistance decreased with increasing RH, but overcoming 40%, nanowire resistance apparently starts to increase. Therefore, two opposite response behaviours were observed at 5–40% and 40–80% which can be ascribed to different dominant sensing mechanisms.

Generally presented sensitivity of RH dependences for n-type semiconducting active elements have linear behaviour in the entire measured RH range with decreasing resistance while increasing the RH [19]. There is also a report for n-type ZnS: Al nanowires possessing maximum in the resistance at RH  $\sim 50\%$  [20] thus showing reverse type behaviour comparing to  $\text{Bi}_2\text{S}_3$  nanowire dependence.

Proposed water molecule sensing mechanisms can be treated from a material point of view—ceramic, semiconducting or nanomaterial [21]. However, for a reasonable explanation of the resistance modulation with the RH we have to consider semiconducting properties and nanometric size. At the low RH level up to 40%, decrease of the nanowire resistance is consistent with response expected for n-type semiconductor. At room temperature surface physisorbed molecules can release free electrons interacting with surface pre-adsorbed oxygen. This mechanism is often discussed for metal oxide nanowire sensors and is considered as electronic sensing. Assuming a thin layer of native oxide  $\text{Bi}_2\text{O}_3$  on top of the  $\text{Bi}_2\text{S}_3$  nanowire surface, which can form at increased temperatures [22] during the sample fabrication, one can expect oxygen promoted water molecule physisorption in the low RH levels. Nanowire surface can also contain a few static adsorbed molecule layers provided by chemisorption, which produce hydroxyl groups [23]. In general, the formation of the SH- groups can be expected for the sulfide surface after interaction with water molecules. However, this effect has not been observed experimentally as a common trend [24]. Therefore, most likely the surface pre-adsorbed oxygen plays a dominating role in formation of chemisorbed water layer. Further increase of the RH (40–80%) causes additional layer adsorption of the water molecules resulting in proton hopping through the water layer.

At RH level 65% and higher, measured response has a unique value of the resistance and it increases nearly linearly with RH. At lower RH values, resistance may have similar values at two different RH levels (e.g. 10% and 60%) Hence, an additional range detector would be required for practical sensor application.

Figure 4 represents dynamic response to the RH. It can be seen, that interaction with water molecules is a reversible

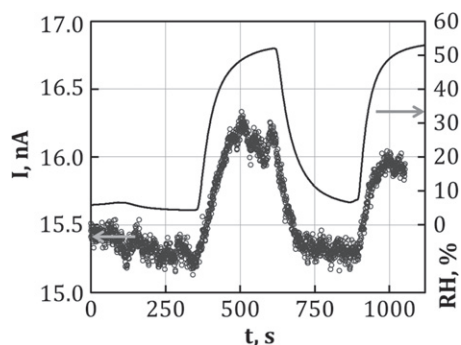


**Figure 4.** Dynamic current switching between different RH levels.

process. Response and recovery time required to achieve 90% of the equilibrium value is  $\sim 50$  and  $60$  s, respectively.

## Conclusions

We have fabricated and characterized individually connected  $\text{Bi}_2\text{S}_3$  nanowire arrays combining dielectrophoresis and lithography techniques. Employing nanowire contact area cleaning during the sample fabrication, a reliable method to produce Ohmic contacts is presented. It was found that individual nanowires exhibit non-monotonous response to the RH indicating on two competing sensing mechanisms at low and high RH levels. Obtained results indicate water molecule impact on the  $\text{Bi}_2\text{S}_3$  nanowire electrical properties.

## Acknowledgments

The work was supported by National Program in Materials Science. GK acknowledges the European Social Fund within the project ‘Support for Doctoral Studies at University of Latvia’.

## References

- [1] Zheng G, Patolsky F, Cui Y, Wang W U and Lieber C M 2005 Multiplexed electrical detection of cancer markers with nanowire sensor arrays *Nat. Biotechnol.* **23** 1294–301
- [2] Zhong Z, Wang D, Cui Y, Bockrath M W and Lieber C M 2003 Nanowire crossbar arrays as address decoders for integrated nanosystems *Science* **302** 1377–9
- [3] Gao X P A, Zheng G and Lieber C M 2010 Subthreshold regime has the optimal sensitivity for nanowire FET biosensors *Nano Lett.* **10** 547–52
- [4] Wang S, Hsiao C, Chang S, Member S and Lam K 2012 CuO nanowire-based humidity sensor *IEEE Sens. J.* **12** 1884–8
- [5] Rau H 1981 Range of homogeneity and defect model *J. Phys. Chem. Solids* **42** 257–62
- [6] Kajokas A, Grigas J, Brilingas A and Banyš J 1999 Origin of anomalies of physical properties in  $\text{Bi}_2\text{S}_3$  crystals *Lith. J. Phys.* **39** 45–53
- [7] Yao K, Gong W W, Hu Y F, Liang X L, Chen Q and Peng L 2008 Individual  $\text{Bi}_2\text{S}_3$  nanowire-based room-temperature  $\text{H}_2$  sensor *J. Phys. Chem. C* **112** 8721–4
- [8] Schricker A D, Sigman M B and Korgel B A 2005 Electrical transport, Meyer–Neldel rule and oxygen sensitivity of  $\text{Bi}_2\text{S}_3$  nanowires *Nanotechnology* **16** S508–13
- [9] Cademartiri L, Scotognella F, Brien P G O, Lotsch B V, Thomson J, Petrov S, Kherani N P and Ozin G A 2009 Cross-linking  $\text{Bi}_2\text{S}_3$  ultrathin nanowires: a platform for nanostructure formation and biomolecule detection *Nano Lett.* **9** 1482–6
- [10] Wang S L, Lin Z X, Wang W H, Kuo C L, Hwang K C and Hong C C 2014 Self-regenerating photocatalytic sensor based on dielectrophoretically assembled  $\text{TiO}_2$  nanowires for chemical vapor sensing *Sensors Actuators B* **194** 1–9
- [11] Pui T S, Agarwal A, Ye F, Balasubramanian N and Chen P 2009 CMOS-Compatible nanowire sensor arrays for detection of cellular bioelectricity *Small* **5** 208–12
- [12] Xu J, Petkov N, Wu X, Iacopino D, Quinn A J, Redmond G, Bein T, Morris M A and Holmes J D 2007 Oriented growth of single-crystalline  $\text{Bi}_2\text{S}_3$  nanowire arrays *Eur. J. Chem. Phys. Phys. Chem.* **8** 235–40
- [13] Erts D, Polyakov B, Daly B, Morris M A, Ellingboe S, Boland J and Holmes J D 2006 High density germanium nanowire assemblies: contact challenges and electrical characterization *J. Phys. Chem. B* **110** 820–6
- [14] Forney C F and Brandl D G 1992 Control of humidity in small controlled- environment chambers using glycerol–water solutions *HortTechnology* **2** 52–4
- [15] Yao K, Zhang Z Y, Liang X L, Chen Q, Peng L-M and Yu Y 2006 Effect of  $\text{H}_2$  on the electrical transport properties of single  $\text{Bi}_2\text{S}_3$  nanowires *J. Phys. Chem. B* **110** 21408–11
- [16] Bao H, Cui X, Li C M, Gan Y, Zhang J and Guo J 2007 Photoswitchable semiconductor bismuth sulfide ( $\text{Bi}_2\text{S}_3$ ) nanowires and their self-supported nanowire arrays *J. Phys. Chem. C* **111** 12279–83
- [17] Birjukovs P, Petkov N, Xu J, Svirskis J, Boland J J, Holmes J D and Erts D 2008 Electrical characterization of bismuth sulfide nanowire arrays by conductive atomic force microscopy *J. Phys. Chem. C* **112** 19680–5
- [18] Tian Y, Guo C F, Guo S, Yu T F and Liu Q 2014 Bivariate-continuous-tunable interface memristor based on  $\text{Bi}_2\text{S}_3$  nested nano-networks *Nano Res.* **7** 953–62
- [19] Leung Y P, Choy W C H and Yuk T I 2008 Linearly resistive humidity sensor based on quasi one-dimensional ZnSe nanostructures *Chem. Phys. Lett.* **457** 198–201
- [20] Jiang P, Jie J, Yu Y, Wang Z, Xie C, Zhang X, Wu C, Wang L, Zhu Z and Luo L 2012 Aluminium-doped n-type ZnS nanowires as high-performance UV and humidity sensors *J. Mater. Chem.* **22** 6856
- [21] Chen Z and Lu C 2005 Humidity sensors: a review of materials and mechanisms *Sens. Lett.* **3** 274–95
- [22] Pejova B, Tanuševski A and Grozdanov I 2005 Photophysics, photoelectrical properties and photoconductivity relaxation dynamics of quantum-sized bismuth(III) sulfide thin films *J. Solid State Chem.* **178** 1786–98
- [23] Morimoto T, Nagao M and Tokuda F 1969 Relation between the amounts of chemisorbed and physisorbed water on metal oxides *J. Phys. Chem.* **73** 243–8
- [24] Ratnasamy P and Fripiat J J 1970 Surface chemistry of sulphides *Trans. Faraday Soc.* **66** 2897–910